

# Enzyme-Based Nanoscale Composites for Use as Active Decontamination Surfaces

By Cerasela Zoica Dinu, Guangyu Zhu, Shyam Sundhar Bale, Gaurav Anand, Philippa J. Reeder, Karl Sanford, Gregg Whited, Ravi S. Kane,\* and Jonathan S. Dordick\*

Perhydrolase S54V (AcT) effectively catalyzes the perhydrolysis of propylene glycol diacetate (PGD) to generate peracetic acid (PAA). PAA is a potent oxidant used for sanitization and disinfection, with broad effectiveness against bacteria, yeasts, fungi, and spores. In this study, active and stable composites are developed by incorporating AcT-carbon nanotube conjugates into polymer and latex-based paint. At a conjugate loading of 0.16% (w/v), the composite generated 11 mM PAA in 20 min, capable of killing more than 99% spores initially charged at  $10^6$  colony-forming units per milliliter.

## 1. Introduction

Peracetic acid (PAA) is a potent oxidant that exhibits excellent and rapid disinfection activity against a broad spectrum of pathogens, such as bacteria, yeasts, molds, fungi, and spores.<sup>[1–3]</sup> As a disinfectant PAA is more effective and is needed at lower concentrations than  $H_2O_2$ ,<sup>[4]</sup> while as a sanitizer PAA has been found to be more effective than chlorine to deactivate biofilms on stainless-steel surfaces.<sup>[5]</sup> PAA can be used over a wide range of temperatures (0–40 °C) and pH (3.0–7.5)<sup>[6]</sup> and it decomposes into nontoxic oxygen, acetic acid, and water. As a result, PAA has been approved by the U.S. EPA as a pesticide and by the FDA for direct food contact and food contact surfaces. PAA has also been used to disinfect medical supplies,<sup>[7,8]</sup> for waste water treatment, and for pulp and textile bleaching.<sup>[9]</sup>

Commercial PAA is generally produced by reacting acetic acid with  $H_2O_2$  using sulfuric acid as the catalyst. However, this reaction is slow (requiring up to several days to yield high amounts of PAA); moreover, residual levels of acetic acid,  $H_2O_2$ , and

corrosive sulfuric acid in the product are high.<sup>[10]</sup> As an alternative to chemical synthesis, several biocatalytic routes have been derived, including the use of lipases, esterases, and cholinesterases. These enzymes catalyze perhydrolysis of acyl substrates in the presence of  $H_2O_2$  to generate peracids under mild reaction conditions.<sup>[11–13]</sup> Lipases in particular are well known to generate peracids in non-aqueous media, which are then able to oxidize alkenes stoichiometrically to generate epoxides and peracids.<sup>[14–16]</sup> For example, Novozyme 435 (lipase B from *Candida antarctica* immobilized on acrylic resin) has been used to generate peracids either by direct synthesis from carboxylic acids and  $H_2O_2$  or by perhydrolysis of carboxylic acid esters.<sup>[17]</sup> The enzymatically produced PAA was found to have sporicidal activity similar to that of commercial PAA. However, the major drawback of using hydrolases is their very low perhydrolytic activity in aqueous solutions and fast deactivation by high concentrations of  $H_2O_2$  and the resulting PAA.

Significant efforts have been made to address the generation of PAA from an aqueous environment through identification of perhydrolases with greater reactivity on  $H_2O_2$  than on water as the acyl acceptor. In particular, perhydrolase S54V (denoted as AcT) from *Mycobacterium smegmatis* is active on various acyl donor substrates and exhibits a perhydrolysis to hydrolysis ratio greater than one. This results in perhydrolase activity 50-fold higher than that of the best lipase tested.<sup>[18,19]</sup>

In the current work, we have exploited AcT interaction with multiwalled carbon nanotubes (MWNTs) to produce bioactive composites that generate PAA by perhydrolysis of propylene glycol diacetate (PGD) in the presence of  $H_2O_2$  (Fig. 1). Our strategy involved covalent attachment of AcT to MWNTs and subsequent incorporation of the resulting conjugates into polymers (poly(methyl methacrylate) (PMMA) and poly(vinyl acetate) (PVAc)), and latex-based paint. MWNTs were chosen as support material due to several intrinsic advantages, including: i) ease of surface

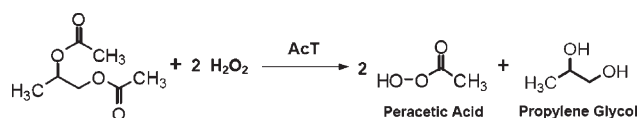


Figure 1. AcT-catalyzed perhydrolysis of PGD to generate peracetic acid (PAA).

[\*] Prof. R. S. Kane, Prof. J. S. Dordick, Dr. C. Z. Dinu, Dr. G. Zhu, S. S. Bale, G. Anand, Dr. P. J. Reeder  
Department of Chemical and Biological Engineering  
Rensselaer Nanotechnology Center and  
Center for Biotechnology & Interdisciplinary Studies  
Rensselaer Polytechnic Institute  
Troy, NY 12180 (USA)  
E-mail: kaner@rpi.edu; dordick@rpi.edu  
Dr. K. Sanford, Dr. G. Whited  
Genencor International  
Palo Alto, CA 94304 (USA)

DOI: 10.1002/adfm.200901388

functionalization,<sup>[20]</sup> ii) very high surface-area-to-volume ratios that afford high enzyme loading without diffusional limitations and facile isolation and purification of enzyme-MWNT conjugates,<sup>[21]</sup> iii) lightweight and yet high mechanical strength<sup>[22]</sup> that make them excellent filling materials to reinforce polymers<sup>[23–25]</sup> and ceramics,<sup>[20,26]</sup> and iv) ensured entrapment of the enzyme, and thus enzyme retention within the composite (with no enzyme leaching). The incorporation of AcT–MWNT conjugates into polymers and paints is the first step in the preparation of bioactive composites with enhanced strength and extended lifetime. These composites may be applied as decontaminating coatings for buildings and environmental remediation or for medical settings where effective killing of a variety of infectious organisms is critical.

## 2. Results and Discussion

### 2.1. AcT–Carbon-Nanotube Conjugates

High activity and good solubility/dispersibility of enzyme–nanotube conjugates are required to construct practically useful bioactive composites. Aggregation of pristine carbon nanotubes in both aqueous and organic solvents due to surface–surface van der Waals interactions reduces available surface areas for biomolecule attachment and also prevents their efficient dispersion in a polymer or paint composite.<sup>[27,28]</sup> To that end, we used functionalized MWNTs that have been oxidized via acid treatment<sup>[29]</sup> yielding free carboxylic acid groups. The acid-functionalized MWNTs were soluble in water up to at least 5 mg mL<sup>−1</sup> following brief sonication.

Covalent attachment of AcT to the water-soluble MWNTs was performed via EDC/NHS chemistry<sup>[30]</sup> (Fig. 2a; see Experimental Section for more details) providing AcT loadings of (0.12 ± 0.01) mg (mean ± standard deviation) AcT per milligram

of MWNTs, as determined by the bicinchoninic acid (BCA) protein assay and elemental analysis. The resulting AcT–MWNT conjugates were soluble to at least 2.5 mg mL<sup>−1</sup> in aqueous buffer (50 mM potassium phosphate, pH 7.1). This solubility was deemed sufficient to provide further uniform dispersion of the conjugates into polymeric and paint composites, which is expected to lead to uniform activity per unit area of the composites by distributing the enzyme conjugates throughout the material.<sup>[23,31,32]</sup>

Contrary to their excellent water dispersity, the AcT–MWNT conjugates only retained about 7% of the native AcT activity. Changing the conditions for AcT immobilization, such as varying the pH of the buffer and using different ratios of AcT/nanotube or EDC/NHS, did not improve bound enzyme activity. This activity was substantially lower than that for other enzymes immobilized onto carbon nanotubes. For example, glucose oxidase (GOx) immobilized onto carbon nanotube retained 68% of the free GOx activity<sup>[33]</sup> while soybean peroxidase (SBP) covalently attached to MWNTs retained around 55% of the free SBP activity.<sup>[21]</sup>

AcT is a large molecule (an octamer,  $M_w = 184$  kDa) with dimensions of 72 × 72 × 60 Å (Fig. 3a) formed through tight association of pairs of dimers. Bioinformatic calculation (performed using ProtParam and images created on MOE, Chemical Computing Group Inc.) revealed that ~60% of the amino acid residues that constitute the monomer are hydrophobic and the average hydrophobicity of the monomer is 0.117 (Supporting Information Fig. S1). Specifically, there are four insertions: residues 17–27, residues 59–69, residues 122–130, and residues 142–156 in the AcT structure (Fig. 3b), which form loops at the dimer interfaces and contribute to stabilization of the octameric structure. These loops enable formation of a hydrophobic channel that extends to the exterior of the octameric surface (Supporting Information Fig. S2). The regions forming the hydrophobic channel lead to the active sites of the AcT being somewhat buried and thus having restricted substrate accessibility.<sup>[18]</sup> Moreover, the large block-like structure and extensive hydrophobicity of AcT

would presumably lead to substantial nonspecific hydrophobic interactions between the AcT surface and the non-functionalized hydrophobic regions of the MWNTs. These nonspecific hydrophobic interactions determine close packing of AcT molecules onto the MWNT surface and potentially bury the hydrophobic catalytic site (Fig. 2a, inset; as a comparison the bare acid-treated MWNTs are also shown). Consequently, the attached AcT molecules would have limited flexibility and their strong interaction with nanotube surface (via hydrophobic–hydrophobic interactions) would reduce the substrate accessibility to the active site and thus the enzyme activity.

Amphiphilic poly(ethylene glycol) (PEG) is a particularly effective linker, which is known to reduce nonspecific interactions,<sup>[34,35]</sup> will not decrease the solubility of the carbon nanotubes,<sup>[36,37]</sup> and can enhance enzyme activity due to improved surface hydrophilicity.<sup>[38]</sup> To this end, a bifunctional amino-dPEG<sub>12</sub>-acid (dPEG, 4.7 nm in contour length) spacer was

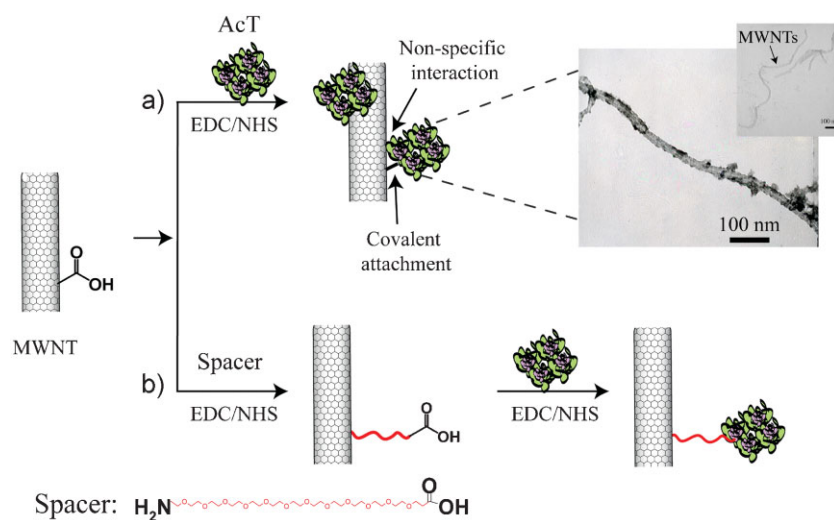


**Figure 2.** Covalent attachment of AcT onto multiwalled carbon nanotubes (MWNTs). a) Direct attachment of AcT onto MWNTs. In addition to covalent binding, nonspecific hydrophobic interaction also occurs due to the large size and hydrophobic nature of AcT. Inset: TEM image of AcT–MWNT conjugates. b) Attachment of AcT onto MWNTs using dPEG as spacer.

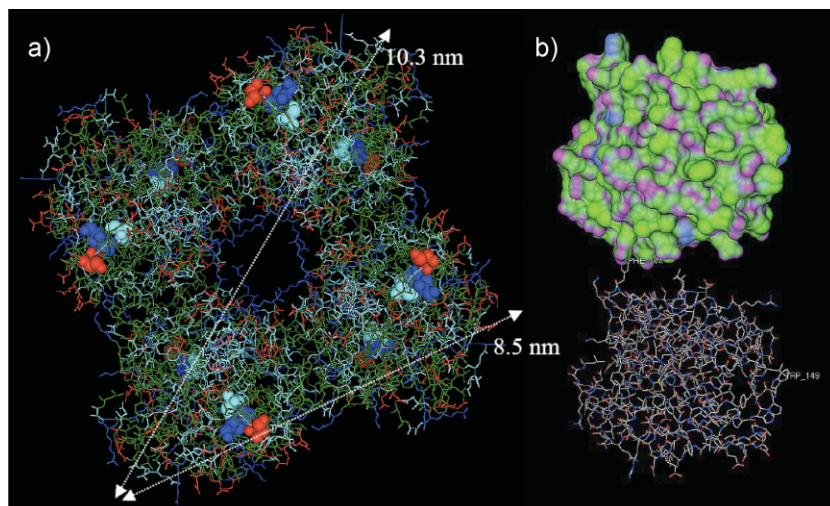


**Figure 3.** Structure of AcT. a) AcT is an octamer with the catalytic triad Ser11, Asp192, and His195 shown in filled space; all other residues are shown with lines where the colored residues indicates green: hydrophobic, pale blue: hydrophilic, dark blue: basic, and red: acidic. b) Molecular surface of monomeric AcT; colored residues, green: hydrophobic, pink: hydrogen bonding, and blue: mild polar.

first covalently attached to the acid treated MWNTs and subsequently AcT was attached to the free end of the spacer—both attachments being performed via EDC/NHS amide formation (Fig. 2b; Supporting information Fig. S3). Attenuated total-reflection Fourier infrared spectroscopy (ATR-FTIR) was used to determine the presence of amide bonds before and after the protein was chemically grafted onto nanotubes (Supporting information Fig. S4). Covalent attachment of PEG to the MWNT surface was confirmed by the presence of amide I band ( $1600\text{--}1700\text{ cm}^{-1}$ , centered at  $1656\text{ cm}^{-1}$ ). Further functionalization of the dPEG–MWNTs with AcT led to additional vibrational stretch ( $1656\text{ cm}^{-1}$ ) and  $\sim 50\%$  increase in the amide bonds arising primarily from carbonyl bond stretching vibrations that formed the protein linkages.<sup>[39]</sup>

The dPEG spacer was effective in increasing the specific activity of the resulting AcT–dPEG–MWNT conjugates to  $\sim 24\%$  of that of free AcT and also in blocking the hydrophobic non-functionalized nanotubes walls thus preventing non-specific enzyme attachment<sup>[35]</sup> (Fig. 4a). Other PEG spacers could be also employed; however, similar effects in terms of blocking non-specific protein binding should be observed.<sup>[40]</sup> Longer spacers ( $>2000$ ), however, are to be avoided, since they could potentially create porous composites and thus alter their mechanical properties.<sup>[41]</sup> When  $0.2\text{ mg mL}^{-1}$  nanotube and  $0.4\text{ mg mL}^{-1}$  AcT were used in the coupling reaction, the resulting AcT–dPEG–MWNT conjugates had an enzyme loading of  $(0.06 \pm 0.02)\text{ mg AcT per mg of nanotube}$  as determined by elemental analysis. These conjugates were soluble up to  $2.5\text{ mg mL}^{-1}$  in aqueous buffer. Kinetic studies were performed for both free AcT and AcT–dPEG–MWNT conjugates by varying the concentration of  $\text{H}_2\text{O}_2$  from  $0.1$  to  $400\text{ mM}$  while maintaining the PGD concentration at  $200\text{ mM}$ . Both free AcT and AcT–dPEG–MWNT conjugates followed Michaelis–Menten kinetics (Fig. 4b) with  $k_{\text{cat}}$  values of  $4.6 \times 10^5$  and  $1.3 \times 10^5\text{ min}^{-1}$  for free AcT and AcT–dPEG–MWNT conjugates, respectively. Thus, the conjugate possessed  $\sim 28\%$  of the intrinsic

catalytic turnover as that of the free enzyme, indicating that the PEG linker markedly improved the reactivity of the enzyme when compared to the direct covalent attachment of the enzyme to the MWNTs. The  $K_m$  values were  $115$  and  $123\text{ mM}$  for free AcT and AcT–dPEG–MWNT conjugates, respectively. Therefore, attachment of AcT onto functionalized MWNT via dPEG spacer did not significantly alter substrate-binding affinity. The good kinetic properties of the AcT–dPEG–MWNT conjugates led us to use this formulation for preparation of the polymer and paint composites.

## 2.2. AcT–dPEG–MWNT Composites

Having established that the AcT–dPEG–MWNT conjugates retained relatively high intrinsic catalytic activity and had high water dispersity, we incorporated the conjugates into two industrially relevant polymers—poly(methyl methacrylate) (PMMA) and poly(vinyl

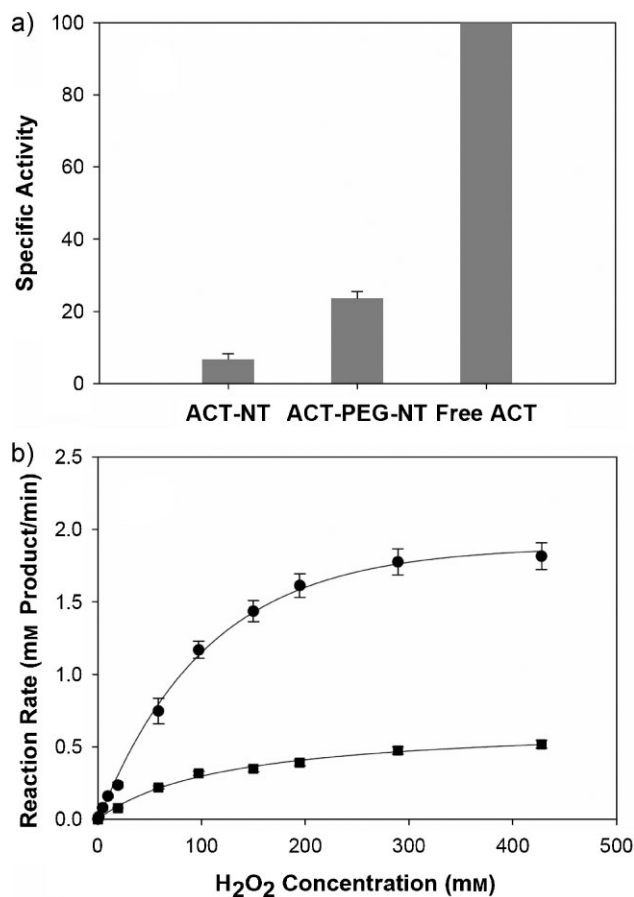


**Figure 4.** a) Specific activity of AcT–nanotube conjugates compared to free AcT. b) Kinetics of free AcT (filled circles) and AcT–dPEG–NT (filled squares) conjugates.

acetate) (PVAc)—and into a latex-based paint. Incorporating biocatalysts into materials has been of interest for more than a decade.<sup>[42–48]</sup> In addition to direct crosslinking of biomolecules into the composite matrix, polymeric composites have also been prepared by interacting enzymes with a third component such as a different polymer,<sup>[49]</sup> activated carbon,<sup>[50]</sup> or carbon nanotubes.<sup>[51,52]</sup> With regard to the latter, we have shown that both single- and multiwalled carbon nanotubes are able to stabilize enzymes in polymer composites,<sup>[51,52]</sup> eliminating the need to crosslink the enzymes within the network.

To prepare polymeric composites, water solutions of AcT-dPEG-MWNT conjugates were added to acetone solutions of PMMA or PVAc at a volume ratio of 1:15 (enzyme-based conjugates:polymer) and mixed by vortexing. The composites were then formed either by direct evaporation of the acetone and water in a glass vial or by spin-coating the solution onto a glass cover slide. The use of acetone as the solvent avoided phase separation encountered by more hydrophobic solvents such as toluene and chloroform, while the initial solubilization of the conjugates in water aided their subsequent dispersion in the polymer solutions without sonication. In the case of paint composites, a 1:10 volume ratio of water solution of AcT-dPEG-MWNT conjugates to latex was used. Visually there was no phase separation for either the polymer or latex-based composites. The two-step process applied in this work also made it convenient to control the composite activity simply by varying the loading of AcT-dPEG-MWNT conjugates.

AcT activity in the PMMA and PVAc composites obtained by direct evaporation was quite low, <10% of that of the AcT-dPEG-MWNT conjugates in aqueous solution (Fig. 5a). However, these polymer films had a thickness of ~200  $\mu\text{m}$ , which could have severely limited the diffusion of the two substrates PGD and  $\text{H}_2\text{O}_2$  to the immobilized AcT. Indeed, estimation of the Thiele Modulus,  $\phi^2$  (Equation 1), for  $\text{H}_2\text{O}_2$  revealed a value of 230 indicating strong diffusional limitations (Thiele Modulus represents the ratio of the intrinsic reaction rate in the absence of mass transfer limitation to the rate of diffusion through the medium).<sup>[53]</sup>

$$\phi^2 = \left(\frac{h}{2}\right)^2 \frac{v_{\max}}{D_{\text{eff}} K_m} \quad (1)$$

In Equation 1,  $h$  is the film thickness (200  $\mu\text{m}$ ) and  $v_{\max}$  is the maximal enzyme reaction rate ( $= k_{\text{cat}} \times \text{enzyme concentration}$ ). We used the value of  $k_{\text{cat}} = 1.3 \times 10^5 \text{ min}^{-1}$  (as found in our kinetic studies above), a  $K_m$  of 123 mM, and the enzyme concentration was obtained from the loading (40  $\mu\text{g}$  conjugate or 2.4  $\mu\text{g}$  of AcT, 184 kDa enzyme molecular weight) in PMMA. The effective diffusivity ( $D_{\text{eff}}$ ) was estimated to be  $10^{-10} \text{ cm}^2 \text{ s}^{-1}$ . This value was based on water diffusion in a PMMA ( $M_w = 834 \text{ kDa}$ ) film at a thickness of 200  $\mu\text{m}$ .<sup>[54]</sup> In addition to the diffusional limitations caused by the thick films, the large molecular size and hydrophobic character of AcT could lead to extensive interaction with the surrounding hydrophobic PMMA and PVAc molecules, which would further limit the accessibility of the substrates to the AcT active sites.

To overcome mass transfer limitations in the polymeric composites, we dramatically reduced the film thickness from 200  $\mu\text{m}$  to ~2  $\mu\text{m}$  by spin-coating the mixed solution of

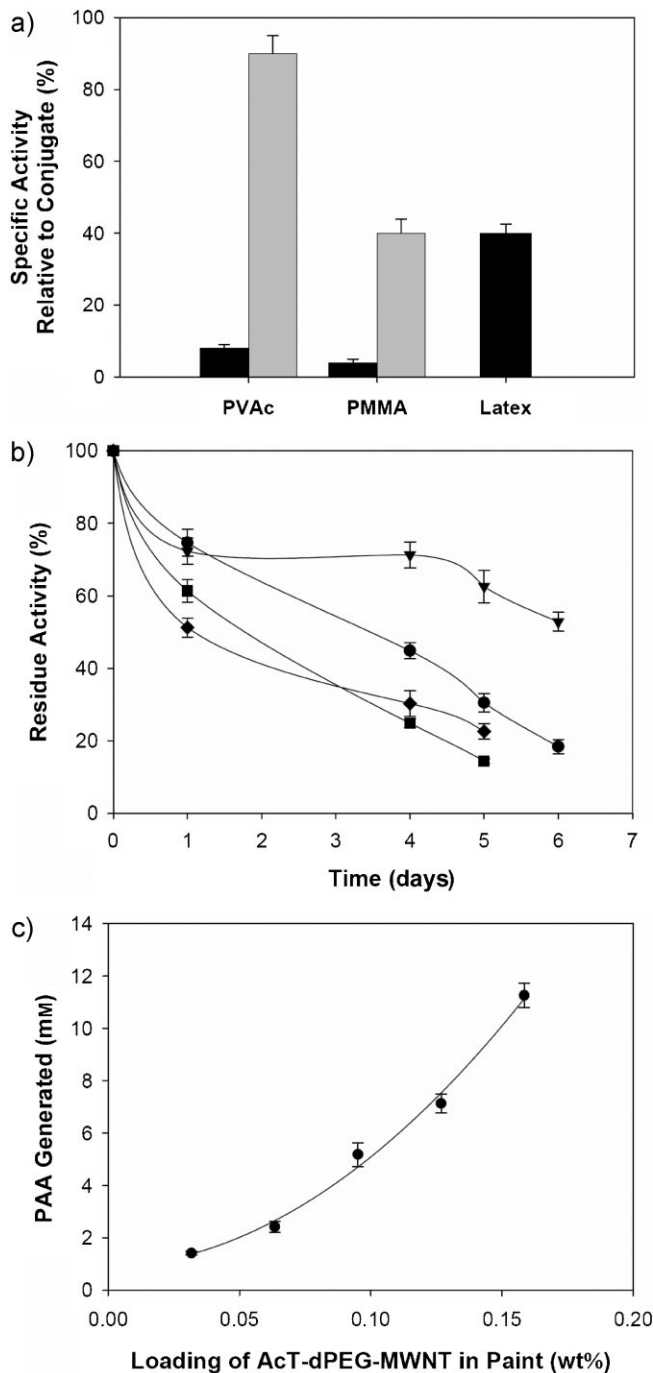


**Figure 5.** a) Specific activity of the composites relative to that of AcT-dPEG-MWNT conjugates. Black bars indicated thick films obtained by direct evaporation (200  $\mu\text{m}$  for polymeric composites and 400  $\mu\text{m}$  for paint composite) and grey bars indicated thin films obtained by spin-coating (~2  $\mu\text{m}$  for polymeric composites). b) Stability of the paint composite tested under different conditions: (●) dry state at room temperature; (▼) immersed in water at room temperature; (■) dry state at 50°C; (◆) immersed in water at 50°C. c) PAA generated in 20 min by paint composite at different loadings of AcT-dPEG-MWNT conjugates. The paint has a surface area of 5  $\text{cm}^2$  and a thickness of around 400  $\mu\text{m}$ . Reactions were conducted in 1 mL potassium phosphate buffer (50 mM, pH 7.1) containing 100 mM  $\text{H}_2\text{O}_2$  and 100 mM PGD.

AcT-dPEG-MWNT conjugate and polymer onto a cover glass (Supporting Information Fig. S5). The corresponding activity of the AcT-dPEG-MWNT polymer films increased to ~40% and more than 90% of the conjugate activity for PMMA and PVAc, respectively (Fig. 5a). The relatively hydrophilic nature of PVAc film may contribute to its higher activity when compared to the more hydrophobic and dense PMMA film. The more porous latex paint composite was not nearly as diffusionally limited as the polymers with ~40% of the conjugate activity even at a thickness of 400  $\mu\text{m}$ .

The MWNT-based composites formulation enabled high retention of the active and stable enzyme in the polymeric film or in paints with no leaching from the composite. In controls, when the enzyme is entrapped in the composite without the MWNT support, >50% of the enzyme is lost from the composite (PMMA, PVAc, or paint) due to leaching in less than 1 h. In other controls, we have immobilized AcT onto silica-based nanoparticles (15  $\pm$  5 nm) by physical adsorption or by covalent binding. For physical adsorption, we incubated directly AcT to nanoparticles with or without *n*-octadecyltrimethoxy silane (*n*-ODMS) functionalization, while for covalent binding we used carboxyl-functionalized nanoparticles and similar immobilization conditions as for MWNTs (Supporting Information). Physical attachment led to high loadings of AcT (~0.05 mg AcT/mg nanoparticle based on the BCA assay); lower loadings were obtained for covalent attachment (~0.03 mg AcT/mg nanoparticles based on the BCA assay). However the physically attached enzyme quickly leached from the polymer or paint composites, presumably due to the weak enzyme-nanoparticle interaction and high porosity of the resultant films. The covalently attached enzyme did not leach out; however, it showed only ~25% of the activity of the AcT-PEG-MWNTs and significant loss of composite enzyme activity occurred. This is in agreement with previous reports that have shown that binding of the enzymes to nanoparticles is strongly affected by size, and hence the surface curvature of the support with the physical property at the nanoscale influencing the stability and unfolding of adsorbed proteins.<sup>[55]</sup> Thus, MWNTs provide a unique material for enzyme incorporation into the polymeric or paint films and lead to composites with active and stable biocatalytic activity, with no enzyme leaching observed.

In addition to composite activity and leaching experiments, we also examined composite stability and reusability. The spin-coated polymer films and the latex paint composites were stored under different conditions and their activity was measured every 24 h. The storage conditions were selected to mimic the environment that could be encountered in real-life applications, and thus included storage in dry state at room temperature and 50°C, and storage in the hydrated state (by immersing the composites in water) at room temperature and 50°C respectively. The paint exhibited high stability when immersed in water at room temperature (Fig. 5b). After a six-day incubation and five reaction cycles, the paint retained >50% of its initial activity. Surprisingly, when stored in dry state at room temperature the paint only enabled ~20% of its original activity after six days and five reaction cycles. A similar trend was also observed at 50°C with a more rapid loss in activity. The unusual result whereby lower enzyme stability was observed in the dry state was rationalized as being due to residual PAA from the enzymatic reaction being retained in the AcT-containing paint. To test this hypothesis, the paints were

incubated in the reaction solution for 1, 2, and 3 h after a typical 20-min reaction. The paints were then rinsed with water and air-dried. After 24 h, the paints retained 75%, 60%, and 30% of their original activity, respectively. This indicates that PAA is able to cause enzyme deactivation. In addition, to evaluate sample-handling effects (e.g., drying and washing) on the activity loss, we also compared the activity of the paint immersed in buffer with that of the paint immersed in the reaction solution after five reaction cycles (one day per cycle). The paint incubated in buffer showed no activity loss while the paint incubated in reaction solution showed a 60% activity loss. We reasoned that the residual PAA was able to diffuse easily out of the paint stored in buffer, and hence cause less deactivation of immobilized AcT. The PVAc and PMMA thin films showed similar stability trends as that of the paint under all testing conditions. When immersed in water, after five days and four reaction cycles the PVAc film retained 53% of its original activity, while after four days and three reaction cycles the PMMA film retained 62% of its original activity.

The ability of these composites to generate PAA is of interest in the development of decontaminating coatings. PVAc thin films (thickness  $\approx$  2  $\mu\text{m}$ , surface area of 5  $\text{cm}^2$ ) containing a conjugate loading of 0.06 wt% (0.004 wt% of AcT) generated 0.2 mM PAA in 20 min; under the same conditions the thin PMMA film generated 0.05 mM of PAA at a conjugate loading of 0.08 wt% (0.005 wt% of AcT). Moreover, the paint composite (thickness  $\approx$  400  $\mu\text{m}$ ) generated > 11 mM PAA at a conjugate loading of 0.16% (0.01 wt% of AcT; Fig. 5c). Even though the polymeric thick films obtained by direct evaporation were diffusion limited, the larger amount of catalyst present (as compared to the spin-coated films) was able to yield higher levels of PAA. It has been reported that PAA is bactericidal at 0.13 mM and fungicidal at 0.39 mM.<sup>[56]</sup> In other tests, PAA was shown to effectively kill bacteria at concentration as low as 0.05 mM<sup>[57]</sup> and reduce spore colony-forming units (CFUs)  $10^{3-5}$ -fold at a PAA concentration of 4 mM.<sup>[6]</sup> Hence, the AcT-based paints would be expected to be highly microbicidal/sporicidal. Indeed, following 20-min incubation of the AcT-containing paint, the supernatant was capable of killing > 99% of *Bacillus cereus* spores initially charged at  $10^6$  CFU  $\text{mL}^{-1}$ . Further investigation is underway to assess the killing efficiency of these composites on different pathogens.

### 3. Conclusions

In summary, highly water-soluble AcT-carbon nanotube conjugates were prepared and uniformly incorporated into polymer films and latex paint. AcT is perhaps the largest enzyme attached to carbon nanotubes (an octameric enzyme with a molecular weight > 180 kDa and dimensions of 72  $\times$  72  $\times$  60 Å) to show activity and stability. Large proteins have an increased surface area that can result in multiple interactions with the support and thus may cause considerable loss of activity. The stability and reusability of the composites was shown to be sufficient for use as a microbicidal and sporicidal decontaminating surface. Moreover, the entanglement of MWNTs in the polymer/paint composite enabled full retention of the nanoscale support. This, in turn, enabled active enzyme to be retained in the composite and is expected to reduce or eliminate potential adverse health effects that could result from release of MWNTs into the environment. Finally,

the capability of generating sufficiently high amount of potent PAA makes these composites useful as coating materials for disinfection.

## 4. Experimental

**Materials:** Perhydrolase S54V (AcT) solution was provided by Genencor International, Inc. (Palo Alto, CA). MWNTs (purity > 95%, outer diameter  $15 \pm 5$  nm, length 5–20  $\mu\text{m}$ ) were purchased from NanoLab, Inc. (Newton, MA). Sulfuric acid ( $\text{H}_2\text{SO}_4$ , 95–98%), nitric acid ( $\text{HNO}_3$ , 68%–70%), and cover glass (circular, 25 mm) were purchased from Fisher Scientific (Hampton, NH). Propylene glycol diacetate (PGD), 2-(*N*-morpholino)ethanesulfonic acid sodium salt (MES), hydrogen peroxide solution (30%), and uranyl acetate were purchased from Sigma (St. Louis, MO). 1-Ethyl-3-[3-dimethylaminopropyl] carbodiimide hydrochloride (EDC) was purchased from Acros Organics (Morris Plains, NJ). BCA protein assay kit, *N*-hydroxysuccinimide (NHS), and (2,2'-azinobis [3-ethylbenzothiazoline-6-sulfonic acid] (ABTS) were purchased from Pierce (Rockford, IL). Isopore filter membrane (pore size 0.2  $\mu\text{m}$ , type GTTP, polycarbonate) was purchased from Millipore (Billerica, MA). Amino-dPEG<sub>12</sub>-acid was purchased from Quanta Biodesign (Powell, OH). Poly(methyl methacrylate) (PMMA, average  $M_w = 996\,000$ ) and poly(vinyl acetate) (PVAc, average  $M_w = 500\,000$ ) were purchased from Aldrich (Milwaukee, WI). Latex enamel (gloss white, manufactured by Yenkin-Majestic Paint Corporation, Columbus, OH) was purchased from a local store.

**Functionalization of Carbon Nanotubes:** Carboxylic acid groups were created on MWNTs by acid treatment. Typically, MWNTs (100 mg) were added to an acid mixture of  $\text{H}_2\text{SO}_4$  and  $\text{HNO}_3$  (45 mL and 15 mL, respectively;  $\text{H}_2\text{SO}_4:\text{HNO}_3 = 3:1$ , v/v) and the suspension was sonicated at room temperature for 6 h in a VWR ultrasonic cleaner (model 50T, frequency from 38.5 to 40.5 kHz, average power of 45 W). The suspension of functionalized MWNTs was then diluted in Milli-Q water (200 mL) and filtered through a 0.2- $\mu\text{m}$  filter membrane. The nanotubes on the membrane were redispersed in Milli-Q water (200 mL) by sonication and filtered again. This process was repeated at least six times to remove residual acids and any solubilized impurities. The functionalized MWNTs were dried under vacuum and stored at room temperature.

**Preparation of AcT–MWNT Conjugates:** AcT was covalently attached to functionalized MWNTs via a two-step process involving EDC/NHS activation followed by enzyme coupling [30]. In a further study, amino-dPEG<sub>12</sub>-acid was used as a spacer between AcT and MWNT. Typically, functionalized MWNTs (2 mg) were dispersed in MES buffer (2 mL, 50 mM, pH 4.7) containing EDC and NHS (160 mM and 80 mM, respectively) by brief sonication. After 15-min shaking at 200 rpm and room temperature, the NHS-activated MWNTs were filtered through 0.2- $\mu\text{m}$  filter membrane and washed thoroughly with MES buffer. NHS–MWNTs were used immediately in the enzyme coupling reaction. For direct enzyme immobilization, NHS–MWNTs (2 mg) were dispersed in potassium phosphate buffer solution of AcT (0.4 mg mL<sup>-1</sup> in 10 mL buffer, 50 mM, pH 7.1) and the enzyme coupling was allowed to proceed for 3 h at room temperature by shaking at 200 rpm. The AcT–MWNT conjugates were filtered and washed extensively with potassium phosphate buffer to remove free enzymes. The AcT–dPEG–MWNT conjugates were prepared by first covalently attaching amino-dPEG<sub>12</sub>-acid (1 mg mL<sup>-1</sup>) to MWNTs and then attaching AcT to dPEG–MWNTs following the two-step process previously described.

**Preparation of Polymer and Paint Composites:** Thin AcT–nanotube polymer films were prepared by spin-coating (spin processor model: WS-400E-6NPP-LITE, Laurell Technologies Corporation, North Wales, PA) the conjugate–polymer solution at 4500 rpm for 50 s on a cover glass. The conjugate–polymer solution was prepared by mixing water suspension of AcT–dPEG–MWNT conjugates and acetone solution of PMMA (0.08 g mL<sup>-1</sup>) or PVAc (0.1 g mL<sup>-1</sup>) by vortexing. The thickness of the polymer films was measured using a profilometer (Dektak 8, Veeco Instruments Inc., Plainview, NY). To prepare thick films, the conjugate–polymer solutions (1 mL) were added in a glass vial (2.5-cm diameter) and the solvents were evaporated under vacuum. The AcT–nanotube-paint

composites were prepared by adding water suspension of AcT–nanotube conjugates into latex-based paint (typically 0.2 mL) in a glass vial (2.5-cm diameter). The two components were mixed thoroughly using a pipette tip and the mixture was air-dried.

**Enzyme Loading:** The concentration of AcT in solutions was measured using the standard BCA protein assay. Briefly, the working reagent was prepared by mixing 50 parts of reagent A with 1 part of reagent B. AcT solution (50  $\mu\text{L}$ ) was added to the working reagent (1 mL) and the mixture was incubated at 37 °C for 30 min followed by measuring the absorbance at 562 nm on a UV–vis spectrophotometer (Shimadzu UV-2401). Serial dilution of AcT was performed to create the calibration curve. The amount of AcT attached on MWNTs was determined by subtracting the amount of enzyme washed out in the filtrates from the amount of AcT initially added. Alternatively, the AcT loading on nanotube was determined by elemental analysis (analyzed by Galbraith Laboratories Inc., Knoxville, TN).

**Activity Assays:** The activity of AcT was determined by measuring the PAA generated [58]. In a typical reaction,  $\text{H}_2\text{O}_2$  stock solution (10.6  $\mu\text{L}$ , final concentration 100 mM) was added to a mixture of PGD solution (0.8 mL, final concentration 100 mM in potassium phosphate buffer, 50 mM, pH 7.1) and AcT solution (0.2 mL, 2.0  $\mu\text{g mL}^{-1}$  final concentration for free AcT or equivalent concentration of AcT for AcT–nanotube conjugates). The mixture was shaken at 200 rpm for 20 min at room temperature. PAA assay was conducted by diluting the reaction solution (25  $\mu\text{L}$ ) 100 times in deionized water and subsequently mixing the diluted solution (25  $\mu\text{L}$ ) with deionized water (75  $\mu\text{L}$ ) and assay reagent (0.9 mL; the assay reagent was prepared by mixing potassium citrate buffer (5 mL, 125 mM, pH 5.0) with ABTS water solution (50  $\mu\text{L}$ , 100 mM) and KI water solution (10  $\mu\text{L}$ , 25 mM)). The mixture was then incubated at room temperature for 3 min and the absorbance at 420 nm was measured on a UV–vis spectrophotometer. PAA concentration was calculated by [Peracetic Acid] (mM) =  $A_{420\text{nm}} \times 0.242 \times 400$  (0.242 is the correlation coefficient between the concentration of PAA and the absorbance at 420 nm, and 400 is the dilution factor). The specific activity of AcT–nanotube conjugates was calculated as the ratio of the normalized activity of the conjugates to that of the native AcT.

The activity of the composites (polymer films and paint) was measured by adding PGD solution (0.8 mL, final concentration 100 mM), buffer (0.2 mL), and  $\text{H}_2\text{O}_2$  solution (10.6  $\mu\text{L}$ , final concentration 100 mM) into the container containing the polymer film or paint. After incubation at room temperature for 20 min, the reaction solution (25  $\mu\text{L}$ ) was withdrawn and PAA assay was conducted as described above. Kinetics of AcT (free AcT and AcT–nanotube conjugates) was studied by measuring the initial reaction rates at different substrate concentrations. The concentration of hydrogen peroxide was varied from 0.1 mM to 428 mM while maintaining the PGD concentration at 200 mM.

**Dispersivity Analysis:** The dispersivity of functionalized MWNT and AcT–nanotube conjugates in water was determined by centrifuging the corresponding water suspension (initial concentration 8 mg mL<sup>-1</sup> for MWNT and 4 mg mL<sup>-1</sup> for AcT–nanotube conjugates) at 3000 rpm for 5 min and then filtering the supernatant (0.8 mL) through a 0.2- $\mu\text{m}$  membrane. After complete drying under vacuum, the amount of MWNT or AcT–nanotube conjugates on the membrane was measured and the dispersivity was calculated based on the volume. It should be noted that the obtained values did not reflect the saturation dispersivity, which is actually the corresponding solubility.

**Sample Imaging:** The morphology of AcT–MWNT conjugates was observed by transmission electron microscopy (TEM) with a field emission gun at 120 kV (Phillips, CM-12). Typically, the conjugate solution in water (10  $\mu\text{L}$ ) was dropped on a Formvar carbon-coated grid (from Electron Microscopy Sciences, Hatfield, PA) and then exposed to a 0.5% solution of uranyl acetate for ~3 s. The samples were vacuum-dried overnight prior to TEM imaging.

## Acknowledgements

C. Z. Dinu and G. Zhu contributed equally to this work. This work was supported by a contract (W911SR-05-0038) from the U.S. Army under a subcontract from Genencor International, and a contract from DTRA

(HDTRA1-08-1-0022). Supporting Information is available online from Wiley InterScience or from the author.

Received: July 27, 2009

Published online: December 15, 2009

- [1] D. M. Portner, R. K. Hoffman, *Appl. Environ. Microbiol.* **1968**, 16, 1782.
- [2] M. G. C. Baldry, *J. Appl. Microbiol.* **1983**, 54, 417.
- [3] D. Small, W. Chang, F. Toghrol, W. Bentley, *Appl. Microbiol. Biotechnol.* **2007**, 76, 1093.
- [4] M. D. J. E. A. S. R. J. W. Lambert, *J. Appl. Microbiol.* **1999**, 87, 782.
- [5] P. Fatemi, J. F. Frank, *J. Food Prot.* **1999**, 62, 761.
- [6] J. L. Sagripanti, A. Bonifacino, *Appl. Environ. Microbiol.* **1996**, 62, 545.
- [7] J. C. Kelsey, I. H. Mackinnon, I. M. Maurer, *J. Clin. Pathol.* **1974**, 27, 632.
- [8] R. O. Richard, A. Ward, *Artif. Organs* **2003**, 27, 1029.
- [9] J. Koivunen, H. Heinonen-Tanski, *Water Res.* **2005**, 39, 4445.
- [10] X. Zhao, T. Zhang, Y. Zhou, D. Liu, *J. Mol. Catal. A: Chem.* **2007**, 271, 246.
- [11] F. Björkling, H. Frykman, S. E. Godtfredsen, O. Kirk, *Tetrahedron* **1992**, 48, 4587.
- [12] O. Kirk, M. W. Christensen, T. Damhus, S. E. Godtfredsen, *Biocatal. Biotransform.* **1994**, 11, 65.
- [13] C. Carboni-Oerlemans, P. Dominguez de Maria, B. Tuin, G. Bargeman, A. van der Meer, R. van Gemert, *J. Biotechnol.* **2006**, 126, 140.
- [14] M. R. g. Klaas, S. Warwel, *J. Mol. Catal. A: Chem.* **1997**, 117, 311.
- [15] M. Rusch gen. Klaas, S. Warwel, *Ind. Crops Prod.* **1999**, 9, 125.
- [16] E. G. Ankudey, H. F. Olivo, T. L. Peeples, *Green Chem.* **2006**, 8, 923.
- [17] M. Rusch gen. Klaas, K. Steffens, N. Patett, *J. Mol. Catal. B: Enzym.* **2002**, 19–20, 499.
- [18] N. S. Amin, M. G. Boston, R. R. Bott, M. A. Cervin, E. M. Concar, M. E. Gustwiller, B. E. Jones, K. Liebeton, G. S. Miracle, H. OH, A. J. Poulouse, S. W. Ramer, J. J. Scheibel, W. Weyler, G. M. Whited, *Perhydrolase*, patent no. WO2005056782 (A2), C12n 9/00 ed.(EdWIPO), Genencor International, Inc. The Procter & Gamble Company, US, **2006**, p. 523.
- [19] I. Mathews, M. Soltis, M. Saldajeno, G. Ganshaw, R. Sala, W. Weyler, M. A. Cervin, G. Whited, R. Bott, *Biochemistry* **2007**, 46, 8969.
- [20] M. O'Connell, *Carbon Nanotubes; Properties and Applications*, 1st Edition, CRC Taylor & Francis, Boca Raton, FL **2006**.
- [21] P. Asuri, S. S. Karajanagi, E. Sellitto, D. Y. Kim, R. S. Kane, J. S. Dordick, *Biotechnol. Bioeng.* **2006**, 95, 804.
- [22] P. M. Ajayan, O. Z. Zhou, *Top. Appl. Phys.* **2001**, 80, 391.
- [23] R. A. E. A. G. B. Safadi, *J. Appl. Polym. Sci.* **2002**, 84, 2660.
- [24] Y. Lin, B. Zhou, K. A. S. Fernando, P. Liu, L. F. Allard, Y.-P. Sun, *Macromolecules* **2003**, 36, 7199.
- [25] L. Qu, Y. Lin, D. E. Hill, B. Zhou, W. Wang, X. Sun, A. Kitaygorodskiy, M. Suarez, J. W. Connell, L. F. Allard, Y. P. Sun, *Macromolecules* **2004**, 37, 6055.
- [26] L. Gao, L. Jiang, J. Sun, *J. Electroceram.* **2006**, 17, 51.
- [27] J. L. Bahr, E. T. Mickelson, M. J. Bronikowski, R. E. Smalley, J. M. Tour, *Chem. Commun.* **2001**, 193.
- [28] S. D. Bergin, V. Nicolosi, P. V. Streich, S. Giordani, Z. Sun, A. H. Windle, P. Ryan, N. P. P. Niraj, Z.-T. T. Wang, L. Carpenter, W. J. Blau, J. J. Boland, J. P. Hamilton, J. N. Coleman, *Adv. Mater.* **2008**, 20, 1876.
- [29] J. Liu, A. G. Rinzler, H. Dai, J. H. Hafner, R. K. Bradley, P. J. Boul, A. Lu, T. Iverson, K. Shelimov, C. B. Huffman, F. Rodriguez-Macias, Y.-S. Shon, T. R. Lee, D. T. Colbert, R. E. Smalley, *Science* **1998**, 280, 1253.
- [30] K. Jiang, L. S. Schadler, R. W. Siegel, X. Zhang, H. Zhang, M. Terrones, *J. Mater. Chem.* **2004**, 14, 37.
- [31] C. A. Mitchell, J. L. Bahr, S. Arepalli, J. M. Tour, R. Krishnamoorti, *Macromolecules* **2002**, 35, 8825.
- [32] S. Bhattacharyya, C. Sinturel, J. P. Salvetat, M. L. Saboungi, *Appl. Phys. Lett.* **2005**, 86, 113104.
- [33] X. Zhao, J. Kim, H. Jia, P. Wang, *Prepr. Symp. - Am. Chem. Soc., Div. Fuel Chem. Chem.* **2007**, 52, 628.
- [34] M. N. C. S. H. B. Klaus Moeschel, *Biotechnol. Bioeng.* **2003**, 82, 190.
- [35] Y. Lin, L. F. Allard, Y. P. Sun, *J. Phys. Chem. B* **2004**, 108, 3760.
- [36] K. A. ShiralFernando, Y. Lin, Y. P. Sun, *Langmuir* **2004**, 20, 4777.
- [37] J. Chattopadhyay, F. deJesusCortez, S. Chakraborty, N. K. H. Slater, W. E. Billups, *Chem. Mater.* **2006**, 18, 5864.
- [38] K. Loos, S. B. Kennedy, N. Eidelman, Y. Tai, M. Zharnikov, E. J. Amis, A. Ulman, R. A. Gross, *Langmuir* **2005**, 21, 5237.
- [39] A. Dong, W. S. Caughey, *Methods Enzymol.* **1994**, 232, 139.
- [40] M. Shim, N. W. S. Kam, R. J. Chen, Y. M. Li, H. J. Dai, *Nano Lett.* **2002**, 2, 285.
- [41] J. Zhao, G. Z. Piao, X. Wang, J. Lian, Z. B. Wang, H. Q. Hu, L. Chen, X. Y. Wang, Y. Tao, D. L. Shi, *Mat. Sci. Eng. C* **2009**, 29, 742.
- [42] P. Wang, M. V. Sergeeva, L. Lim, J. S. Dordick, *Nat. Biotechnol.* **1997**, 15, 789.
- [43] S. J. Novick, J. S. Dordick, *Chem. Mater.* **1998**, 10, 955.
- [44] A. B. Iqbal Gill, *Biotechnol. Bioeng.* **2000**, 70, 400.
- [45] J. Kim, T. J. Kosto, II, J. C. Manimala, E. B. Nauman, J. S. Dordick, *AICHE J.* **2001**, 47, 240.
- [46] N. Vasileva, T. Godjevargova, V. Konsulov, A. Simeonova, S. Turmanova, *J. Appl. Polym. Sci.* **2006**, 101, 4334.
- [47] C. S. McDaniel, J. McDaniel, M. E. Wales, J. R. Wild, *Prog. Org. Coat.* **2006**, 55, 182.
- [48] X. Tong, A. Trivedi, H. Jia, M. Zhang, P. Wang, *Biotechnol. Prog.* **2008**, 24, 714.
- [49] I. Gill, E. Pastor, A. Ballesteros, *J. Am. Chem. Soc.* **1999**, 121, 9487.
- [50] C. Torras, V. Torne, V. Fierro, D. Montane, R. Garcia-Valls, *J. Membrane Sci.* **2006**, 273, 38.
- [51] K. Rege, N. R. Raravikar, D.-Y. Kim, L. S. Schadler, P. M. Ajayan, J. S. Dordick, *Nano Lett.* **2003**, 3, 829.
- [52] P. Asuri, S. S. Karajanagi, R. S. Kane, J. S. Dordick, *Small* **2007**, 3, 50.
- [53] H. W. Blanch, D. S. Clark, *Biochemical Engineering*, Marcel Dekker, Inc, New York **1997**.
- [54] I. Ordaz, L. Singh, P. J. Ludovice, C. L. Henderson, *Mater. Res. Soc. Symp. Proc.* **2006**, 899E, 0899.
- [55] W. Shang, J. H. Nuffer, J. S. Dordick, R. W. Siegel, *Nano Lett.* **2007**, 7, 1991.
- [56] F. P. Greenspan, D. G. MacKeller, *Food Technol. (Chicago, IL, U.S.)* **1951**, 5, 95.
- [57] G. D. L. F. Z. S. Stampi, *J. Appl. Microbiol.* **2001**, 91, 833.
- [58] U. Pinkernell, H.-J. Lüke, U. Karst, *Analyst* **1997**, 122, 567.